

University of California Riverside

ME170B Experimental Techniques: Lab 8

SONIC ANEMOMETER

Group A5

Elijah Perez | Soham Saha | Alex Pham

Fall 2024 - Mon-Wed 8 AM Session

November 8<sup>th</sup>, 2024

**Abstract:**

The purpose of this experiment is to understand the operational principles of a sonic anemometer along with a conceptual understanding of turbulent intensities, Reynolds Stresses, and turbulent heat flux in a controlled setting. It is hypothesized that increasing the thermal energy of air will cause a proportional increase in turbulent intensities, Reynolds stresses, and turbulent heat flux by enhancing airflow instability and turbulence. The study utilized a three-axis sonic anemometer to capture data on three velocity components (x, y, z) along with temperature under three heating conditions (ambient, 1 W heating, and 2 W heating). The ambient room temperature condition served as a baseline, while the additional heat conditions (1 W and 2 W) introduced controlled increases in thermal energy, influencing turbulent flows. Calculations were performed for average velocity components, mean air velocity, and temperature to better understand the fluid dynamics at each heating level. Results of the experiment indicate that turbulent intensity increased significantly as the heating intensity increased, moving from a baseline of 0.2687 at 0 W to 1.3155 at 2 W, and reaching 4.9084 at 1 W. Similarly, heat flux [ $\text{kJ/m}^2\text{s}$ ] exhibited a marked increase, starting at 0.0013 (0 W), rising to 0.8158 (2 W), and peaking at 6.9332 (1 W). These findings underscore the influence of thermal inputs on turbulence dynamics and validate the use of a sonic anemometer for detailed analysis of turbulent flow properties under varying heat conditions.

**Introduction:**

Understanding wind velocities and their sensitivity to temperature changes is crucial for high-performance systems sensitive to turbulent effects, especially in applications involving high-speed military weaponry and advanced aircraft. Variations in wind speed can induce turbulence, impacting aerodynamics, stability, and control, making it essential to explore these dynamics in detail. Researchers often use sonic anemometers to measure wind speed, turbulence, and temperature due to their high precision and real-time data collection capabilities. A sonic anemometer operates by emitting ultrasonic sound waves between paired transducers. These transducers alternate as transmitters and receivers, sending pulses of sound waves through the air. Sound travels omnidirectionally, and thus the travel time of each pulse depends on several factors: the distance between the transducers, the speed of sound in the medium, and the airspeed itself. Changes in wind speed affect the travel time, allowing the anemometer to calculate the velocity components in the x, y, and z directions.

The hypothesis is that increasing the air temperature will lead to higher wind velocities and increased turbulence, reflected in higher turbulent intensities, Reynolds stresses, and turbulent heat flux values. The objectives of this experiment included calculating essential aerodynamic parameters: average velocity components, mean air velocity, mean temperature, turbulent intensities, Reynolds stresses, and turbulent heat flux. These values were derived from the recorded velocity and temperature data obtained through the sonic anemometer and a custom LabView program designed to continuously log this data. To examine the effects of temperature changes on airflow and turbulence, a heating unit was incorporated into the setup. Measurements

were taken at different heating levels to observe how thermal variations influenced wind velocity and turbulence, the unsteady movement of air particles, within the system. Statistical and mathematical analysis was applied to the data, allowing for precise calculation of each parameter. This experiment highlights the importance of accurately measuring and analyzing turbulent airflows in response to temperature fluctuations. Such insights are essential for designing and improving high-speed aerodynamic systems, ensuring both safety and performance. Through this study, the sonic anemometer proved to be an invaluable tool in capturing complex interactions between temperature and wind speed, enabling a deeper understanding of the effects of thermal dynamics on turbulent airflow.

### Theory and Analysis

A sonic anemometer is a precise instrument designed to measure airflow by analyzing the time it takes for a sound pulse to travel from one transducer to another. The travel time of the pulse varies based on three primary factors: the measured distance between the transducers, the air velocity, and the speed of sound through the air, which in turn depends on air temperature. By arranging three sensor pairs along three orthogonal axes, the anemometer can accurately determine the magnitude and direction of the airflow.

$$I = \frac{u'_{rms}}{\bar{u}} = \frac{\sqrt{\frac{1}{3}(\bar{u}'^2 + \bar{v}'^2 + \bar{w}'^2)}}{\sqrt{(\bar{u}^2 + \bar{v}^2 + \bar{w}^2)}} \quad (1)$$

Where :

$$u' = u - \bar{u}$$

$$v' = v - \bar{v}$$

$$w' = w - \bar{w}$$

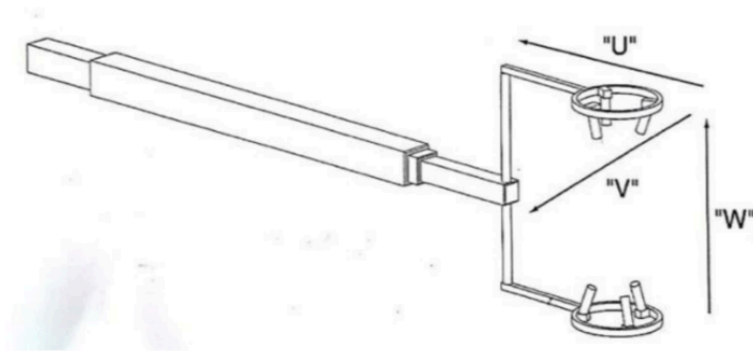


**Figure 1:** Axis directions for “A” type sonic anemometer

The flow of air causes shear stresses, known as Reynolds Stresses. Reynolds Stresses can be calculated for each axis in the case of a three-axis sonic anemometer. The stresses are parallel to the plane normal to the axis and can be found using the equations below:

$$\tau_{u'v'} = \rho \overline{u'v'} \quad (2)$$

$$\tau_{u'w'} = \rho \overline{u'w'} \quad (3)$$

$$\tau_{v'w'} = \rho \overline{v'w'} \quad (4)$$

The turbulent flow is able to cause a heat flux because air is being moved around. The turbulent heat flux quantifies the amount of heat that flows due to the turbulent flow:

$$H = \rho C_p \overline{w'T'} \quad (5)$$

## **Methods:**

### Precautions:

Be careful of the hot plate that will be placed at the bottom of the sonic anemometer for it will be hot and could cause severe burns to the user. Stay clear from the anemometer when collecting data for slight movements will cause fluctuations within the data.

### Calibration of the psychrometer:

Before beginning the calibration process, ensure that the psychrometer is powered off. With the meter off, insert the sensor into the HR 33 salt bottle and leave it for approximately one hour to allow the reading to stabilize. After this stabilization period, initiate calibration by turning on the meter and holding the °C/°F button. The meter will display a flashing 32.8% value, which will become steady when this initial calibration step is complete. While the meter remains on, transfer the sensor to the HR 75 salt bottle, again allowing it to stabilize for about one hour. Once the reading has settled, press and hold the MN/MX button for a few seconds to put the meter into calibration mode. The meter will remain in calibration mode for approximately 30 minutes, during which it completes the calibration process internally. After this period, the meter can be removed from the salt bottle and is now ready to calibrate the anemometer

program. This thorough calibration procedure ensures the psychrometer's readings are accurate and reliable, providing a solid baseline for precise measurements during anemometer calibration.

#### Procedure:

Calibration of the sonic anemometer is essential before collecting accurate measurements. To begin, cover the anemometer's sensors with a zero-air chamber to eliminate any external air interference, ensuring a stable environment for calibration. Once prepared, open the HyperTerminal program for the anemometer and press the ESC key to access the main menu. Select option D to initiate calibration, then confirm by pressing Y.

For the next step, use the psychrometer to measure and record the relative humidity (RH%) and temperature ( $^{\circ}\text{C}$ ). Input these values into the program as they are critical for establishing baseline conditions. The final calibration requirement involves specifying the axes for measurement U, V, and W, which correspond to the three-dimensional velocity components in this setup.

After calibrating, configure data storage by navigating to the "Transfer" tab, and then selecting "Capture Text." This option will prompt you to designate a file location for storing recorded data. To begin the experiment, press 0 in the main menu, initiating data collection. Data will be gathered in three stages: the anemometer will first run for 30 minutes with no applied heat, establishing baseline readings. Following this, the system will be run at two heating levels 1 and 2 for 15 minutes each, allowing for the observation of temperature's effects on airflow and turbulence.

To end each experimental stage, press the "ESC" key to stop data collection. Once all data has been collected, ensure the heating unit is powered off. This thorough calibration and testing procedure ensures that the anemometer provides accurate and reliable measurements across different environmental conditions, allowing for detailed analysis of airflow dynamics.

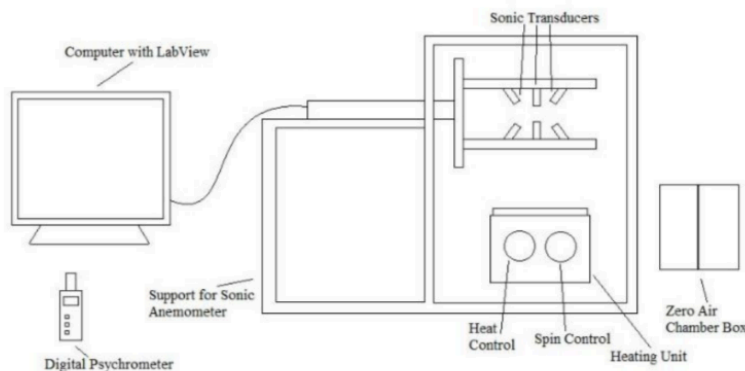


**Figure 2:** Sonic anemometer setup with main components listed

## Results:

In the analysis presented in Figure 4-15, we calculated the mean air velocity components (U, V, W in m/s) and mean temperature (T in °C) for each heat setting: no heat, heat setting 1, and heat setting 2. Table 1 summarizes these results, showing that while the U and V direction velocities remained relatively stable across the heat settings, the W-direction velocity component significantly increased.

	Uavg [m/s]	Vavg [m/s]	Wavg [m/s]	T[degree C]
No Heat	0.0837	0.0105	-0.0325	23.3
Heat 1	-0.02	-0.037	0.235	31.1
Heat 2	0.0355	-0.0176	0.14333	27.7

**Table 1:** Mean air velocity components for various heat settings

Specifically, there was an 836.9% rise in W-direction velocity for heat setting 1 and a 552.1% increase for heat setting 2, indicating a notable response in vertical air movement with the addition of heat. This increase in vertical velocity demonstrates the effect of thermal input on airflow dynamics, suggesting that added heat promotes convective air movement, which has implications for applications where airflow control is critical, such as ventilation and thermal management systems.

The analysis also revealed that the Reynolds stresses ( $\tau_{uv}$ ,  $\tau_{uw}$ ,  $\tau_{vw}$  in N/m<sup>2</sup>) increased consistently with the introduction of heat, reflecting how thermal input disrupts airflow stability by increasing turbulence. Turbulent intensities were recorded at 0.2687 (no heat), 4.9084 (heat setting 1), and 1.3155 (heat setting 2), while turbulent heat flux values (kJ/m<sup>2</sup>s) were calculated at 0.0013, 6.9332, and 0.8158, respectively. These results are summarized in Table 2.

	$\tau_{uv}[N/m^2]$	$\tau_{uw}[N/m^2]$	$\tau_{vw}[N/m^2]$	I	H[kJ/m2s]
No Heat	0.0009	0.0006	0.0006	0.2687	0.0013
Heat 1	1.6857	1.6671	1.6297	4.9085	6.9332
Heat 2	0.0550	0.0437	0.0361	1.3155	0.8158

**Table 2:** Calculated Reynolds stresses, Turbulent Intensities, and Turbulent Heat Flux

It was expected that heat setting 2 should have produced a higher increase in turbulent intensity and heat flux than heat setting 1, which would align with the hypothesis that more heat leads to greater turbulence. However, due to a procedural error in the experiment's sequencing, heat setting 2 was initially applied without allowing sufficient time for ambient air to reach a new thermal equilibrium, the turbulence and thus heat flux measurements did not scale linearly with increased heat. This discrepancy suggests that our hypothesis on linear scaling with heat input may not hold under conditions where thermal equilibrium isn't maintained.

It is also crucial to recognize the many sources of uncertainty associated with this experiment in addition to the procedural error. One major source of uncertainty is the measurement of distance between the transducers on the anemometer. This measurement was completed with a ruler and may not exactly reflect the distance traveled by sound waves between the transducers. Another source of uncertainty is baseline measurements completed using the zero air chamber. While the zero air chamber reduces the impact of ambient convection currents in the room, it does not completely erase all effects, resulting in another source of uncertainty. Additionally, the baseline measurements (no heat addition) can still be influenced by ambient temperature and convection conditions inside of the laboratory.

### **Discussion:**

The results of the experiment indicate that increasing thermal energy does have an effect on turbulent intensity but does not give enough information to determine the exact relationship between thermal energy and increased turbulent intensities, Reynolds stresses, and turbulent heat flux values. Due to the major procedural error previously discussed and the associated unexpected results, the hypothesis for this experiment cannot actually be proven true. While this does not prove the hypothesis invalid, the true validity of the hypothesis remains unknown.

This misalignment underscores the importance of allowing adequate time for temperature stabilization in future experiments to ensure consistent measurement conditions across varying heat settings. Consequently, the reduction to heat setting 1 after initially applying heat setting 2 led to anomalously high readings in turbulent intensity and heat flux, as observed in the recorded data. Furthermore, uncertainties in measurement could have impacted the data, including potential inaccuracies in temperature readings and sensor placement. These errors might have contributed to the unexpected results in turbulent intensity and heat flux, particularly as minor variations in temperature can significantly affect airflow properties in thermally sensitive environments. Addressing these limitations, such as introducing longer waiting times for thermal stabilization and calibrating sensors more precisely, could improve result reliability. In summary, our findings suggest that the added heat significantly impacts vertical airflow dynamics and turbulence, though the results also reveal the limitations of the experiment due to sequencing and thermal equilibrium constraints. Future work should consider these factors to accurately capture the relationship between heat settings and airflow stability, providing more precise data to

support or refine our initial hypotheses about the linearity of turbulence response to thermal inputs.

### **Conclusion & Recommendations:**

This experiment examines the influence of temperature on air movement and demonstrates how a sonic anemometer utilizes sound waves to measure the speed of rising air. As air is warmed, it creates an upward draft, causing the anemometer to register increased air velocity. The experimental setup, which includes measurements along multiple axes, enhances the precision of these readings by capturing airflow data in three-dimensional space, resulting in more reliable averages across all recorded values. One key variable derived from this data is the turbulent heat flux, which reflects the relationship between wind speed and temperature. By analyzing turbulent heat flux, we can better understand how temperature changes impact the dynamics of airflow. During the experiment, the increase in air velocity in the W-direction (vertical) and the rise in turbulent intensities and heat flux confirmed that heating creates significant upward airflow. However, the results revealed an unexpected anomaly: heat setting 1 showed a greater increase in turbulent intensity and heat flux than heat setting 2. This discrepancy raised concerns about the experimental procedure.

As discussed, the main issue in this experiment stemmed from the sequence in which data was collected. Measurements were initially taken at heat setting 2, followed by heat setting 1. This sequence did not allow adequate time for the surrounding air to reach a stable temperature before data collection, nor did it permit the air to cool sufficiently when switching to the lower heat setting. As a result, the readings at heat setting 1 likely reflected residual thermal effects from the higher temperature, thus skewing the measurements. To improve the accuracy of future experiments, it is recommended to begin with the lower heat setting and gradually increase it to the higher setting. Allowing sufficient time for the surrounding air to stabilize at each temperature will ensure more accurate data collection and clearer insights into the relationship between temperature and air movement. This adjustment in protocol will not only produce more reliable measurements but also reinforce the effectiveness of using sonic anemometry to study thermally induced airflow dynamics.

### **Statement of Contributions:**

Elijah Perez: Theory, Experimental Design, Data Analysis, Lab Report

Soham Saha: Data Collection, Lab Report

Alex Pham: Experimental Design, Data Collection



**References:**

- [1] [https://www.cfd-online.com/Wiki/Turbulence\\_intensity](https://www.cfd-online.com/Wiki/Turbulence_intensity)
- [2] Thermal-Fluid Sciences by Cengel and Turner (2nd edition) Ch. 14
- [3] White, Frank. "Fluid mechanics Ch4. differential relations for the fluid particles"
- [4] <https://www.esrl.noaa.gov/psd/data/obs/instruments/SonicAnemometer.pdf>.

## Appendix:

**I** = turbulent intensity

**u'rms** = root mean square of velocity fluctuations

**u'** = velocity in x-direction

**u** = mean velocity in the x-direction

**v'** = velocity in y-direction

**v** = mean velocity in y-direction

**w'** = velocity in z-direction

**w** = mean velocity in z-direction

**$\tau$**  = Reynolds shear stress component

**$\rho$**  = air density

**H** = turbulent heat flux

**Cp** = air heat capacity

**T'** = temperature

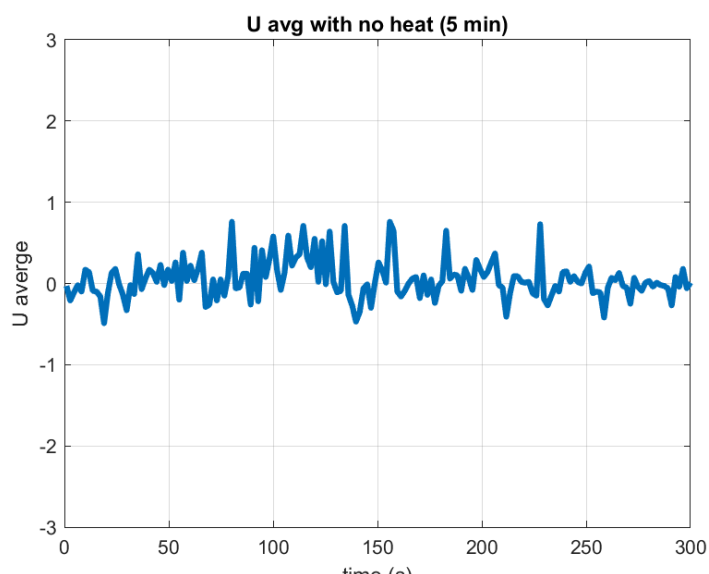


**Figure 3:** No Heat velocity component U vs time (5 minutes)

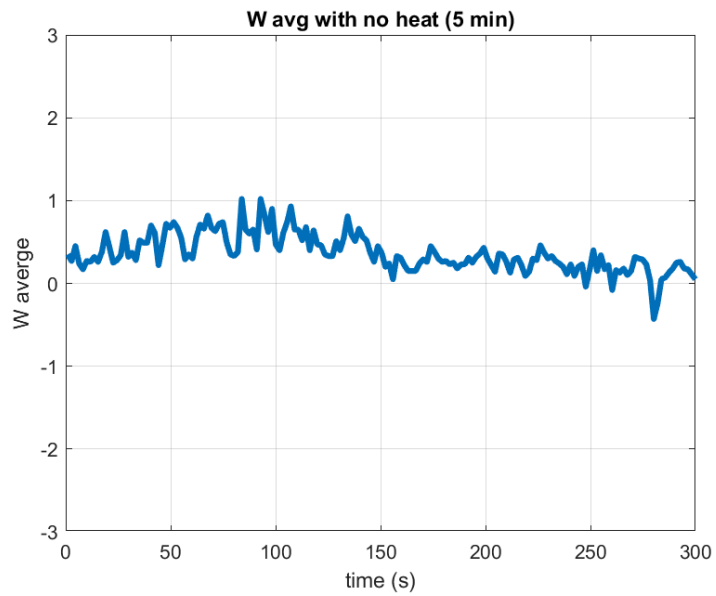


**Figure 4:** No Heat velocity component W vs time (5 minutes)

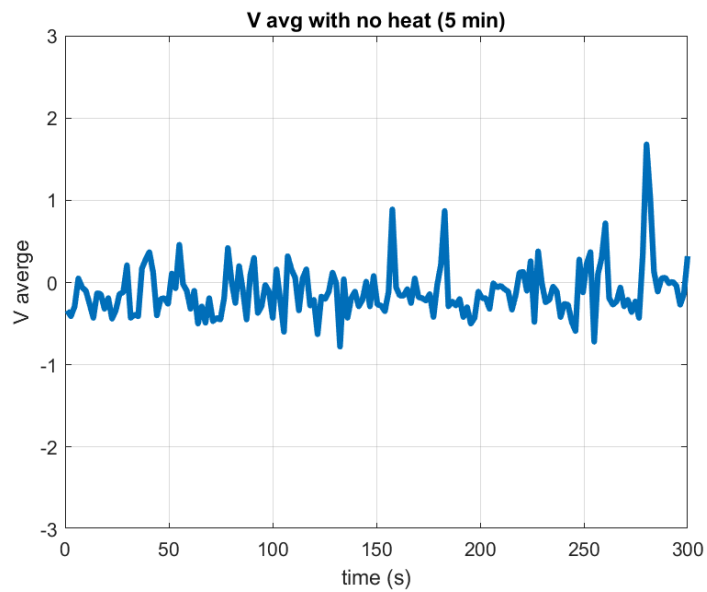


**Figure 5:** No Heat velocity component  $V$  vs time (5 minutes)

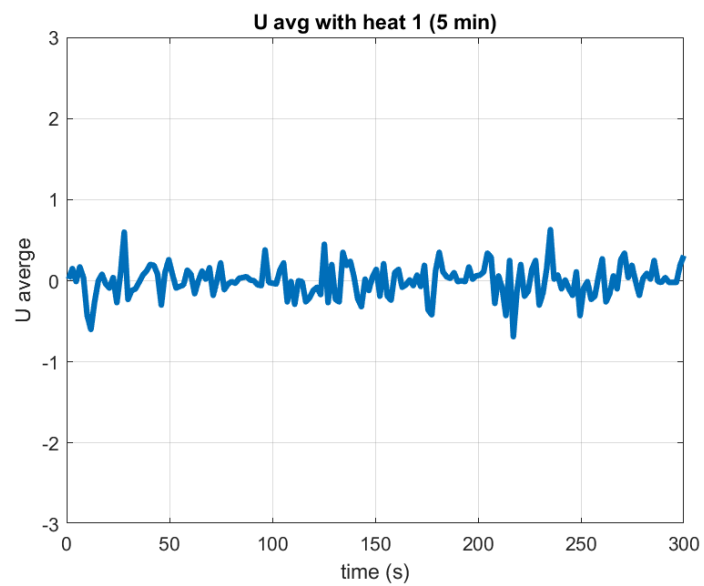


**Figure 6:** Heat 1 velocity component  $U$  vs time (5 minutes)

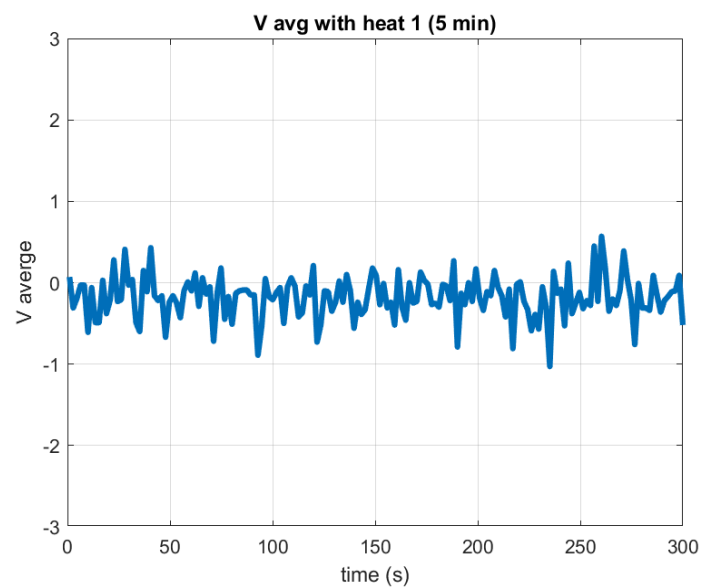


**Figure 7:** Heat 1 velocity component V vs time (5 minutes)

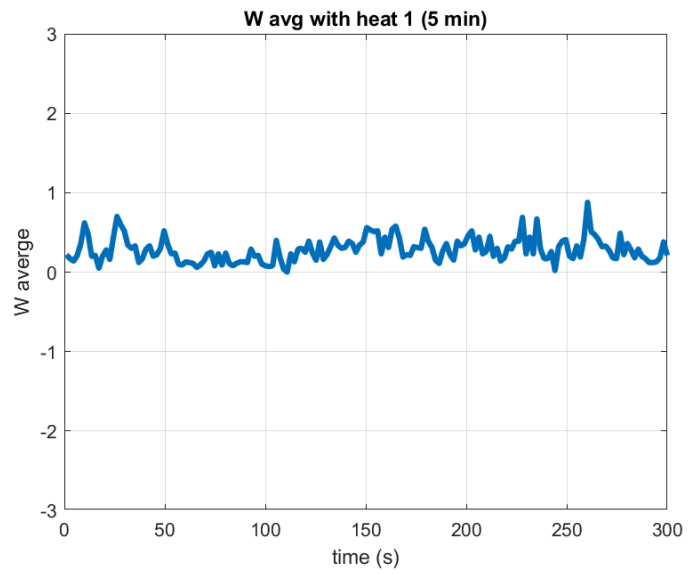


**Figure 8:** Heat 1 velocity component W vs time (5 minutes)

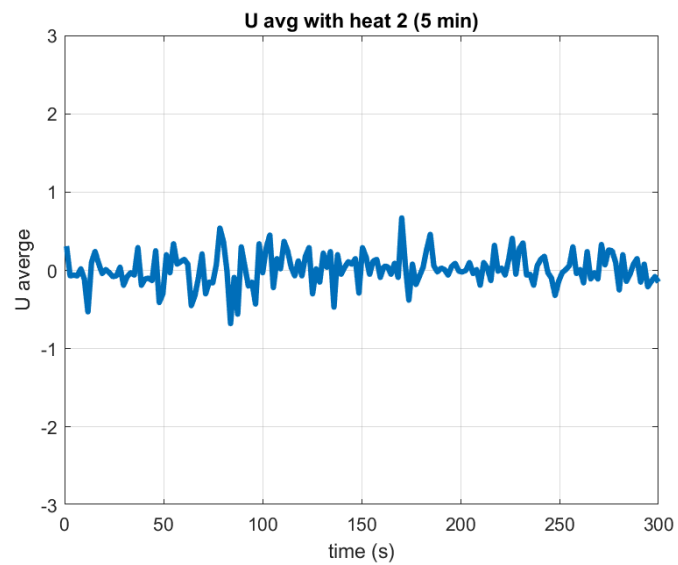


**Figure 9:** Heat 2 velocity component U vs time (5 minutes)

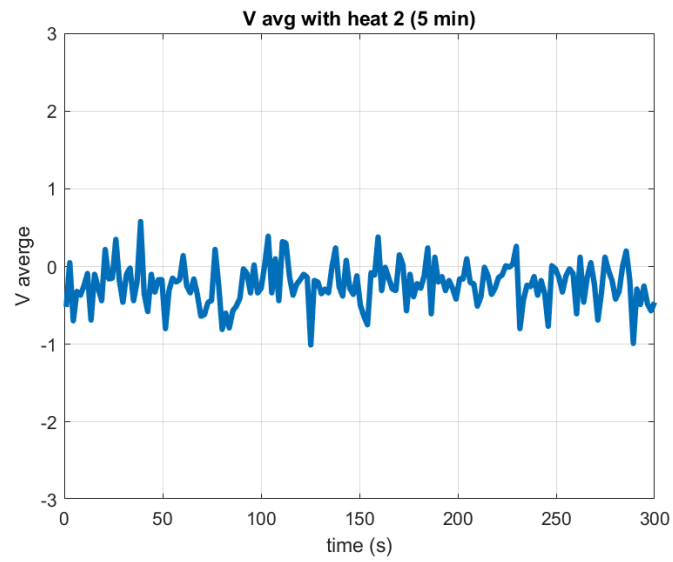


**Figure 10:** Heat 2 velocity component V vs time (5 minutes)

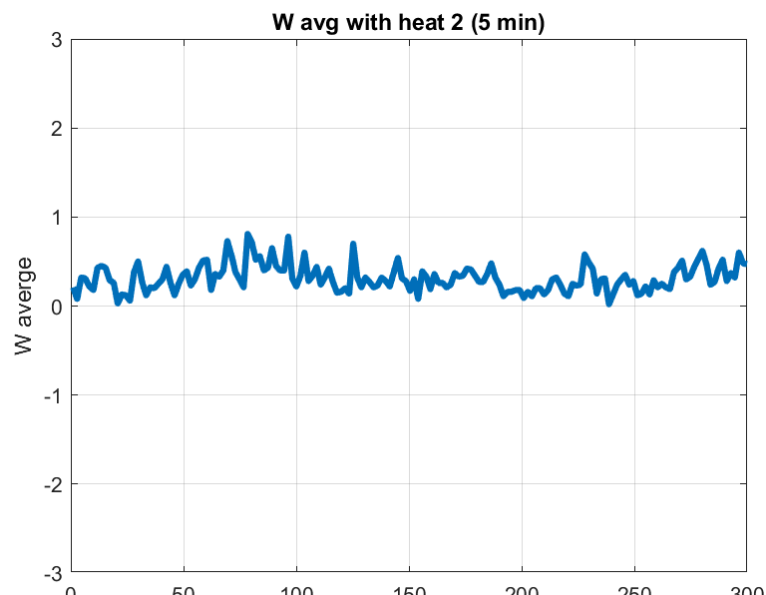


***Figure 11:*** Heat 2 velocity component  $V$  vs time (5 minutes)